Transient localization in the kicked Rydberg atom

Emil Persson,[1] S. Fürthauer,[1] S. Wimberger,[2] and J. Burgdörfer[1]
[1]*Institute for Theoretical Physics, Vienna University of Technology, A-1040 Vienna, Austria*
[2]*CNR-INFM, Dipartimento di Fisica "Enrico Fermi," Largo Pontecorvo 3, I-56127 Pisa, Italy*
(Received 28 April 2006; revised manuscript received 31 July 2006; published 22 November 2006)

We investigate the long-time limit of quantum localization of the kicked Rydberg atom. The kicked Rydberg atom is shown to possess in addition to the quantum localization time τ_L a second crossover time t_D where quantum dynamics diverges from classical dynamics towards increased instability. The quantum localization is shown to vanish as either the strength of the kicks at fixed principal quantum number or the quantum number at fixed kick strength increases. The survival probability as a function of frequency in the transient localization regime $\tau_L < t < t_D$ is characterized by highly irregular, fractal-like fluctuations.

DOI: 10.1103/PhysRevA.74.053417 PACS number(s): 32.80.Rm, 05.45.Mt, 72.15.Rn, 05.45.Df

I. INTRODUCTION

The quantum mechanics of classically chaotic few-degrees-of-freedom systems has become intensively studied in the field of "quantum chaos" [1,2]. One key feature is quantum localization—i.e., the localization of the quantum wave function while the corresponding classical distribution shows diffusion [1–3]. In periodically driven systems, this effect has primarily been studied in the kicked rotor—e.g., [4–7]—and in the Rydberg atom in a sinusoidal electric field—e.g., [8–13]. For both systems, quantum localization is closely related to Anderson localization in transport in disordered systems [2,5,11]. One signal of this analogy is strong fluctuations in the quantum system for different observables when varying some external parameter. A third system experimentally and theoretically studied is the periodically kicked Rydberg atom (e.g., [14–23])—i.e., a hydrogenlike atom prepared in a high-lying state and subjected to a sequence of ultrashort impulses. In a recent publication, we showed the existence of quantum localization in the positively kicked Rydberg atom [24]—i.e., the hydrogenic system with the initial state prepared in a highly elongated quasi-one-dimensional state localized on one side of the nucleus and the periodic impulsive momentum transfer $\Delta p > 0$, pushing the electron away from the nucleus. The classical phase space of this system is globally chaotic with all tori destroyed for arbitrarily small Δp, and the classical survival probability decays algebraically, $P_{\mathrm{sur}} \propto t^{-\alpha}$, with $\alpha \approx 1.5$ (see Fig. 1 and [18]). In contrast, by following the time-dependent system up to a few thousands of kicks we could show both the quantum suppression of classical ionization and the "freezing out" of the wave function, the hallmarks of quantum localization. Several issues remained open, however. They include (i) the origin of a slow, yet noticeable, decay of the localized states, (ii) the dynamical role of high harmonics (up to infinity) present in the system, and (iii) the properties of strong fluctuations present in the localization regime.

In the following paper we address these issues. We identify two characteristic time scales ("break times") in this system. In addition to the localization time τ_l, where quantum and classical dynamics begin to differ from each other due to universal destructive interferences, there is a second break time τ_D where localization is broken. Beyond τ_D, a second crossover occurs where the classical dynamics becomes more stable. This second crossover in the kicked atom is related to the presence of nonclassical photoionization.

In the next section, Sec. II, we describe the method used in our studies, and in Sec. III we show that quantum localization in the kicked Rydberg atom is transient. Strong fluctuations in the survival probability as a function of frequency for fixed times are studied in Sec. IV, and in the last section (Sec. V) a summary is given.

II. METHOD

The Hamiltonian of the one-dimensional (1D) kicked Rydberg atom is (in atomic units)

$$H(t) = H_0 - q\Delta p \sum_{k=1}^{K} \delta(t + T/2 - kT), \tag{1}$$

where $H_0 = \frac{p^2}{2} - \frac{1}{q}$ is the hydrogen Hamiltonian and q the position of the electron. Δp and T are the strength and period of the train of kicks, respectively. We will use the number K of kicks and time $t = KT$ interchangeably. The restriction to a 1D model in the present context is necessary since the study of the long-time limit in 3D is currently computationally not feasible. Our previous studies for up to 10^3 kicks have shown that the 1D model can reproduce essential features of the 3D problem. For a more detailed discussion of the relation between the 1D model and real 3D dynamics, see [24] and references therein. In the case $\Delta p > 0$—i.e., the kicks directed away from the nucleus—the classical phase space is void of stable islands and the effect of quantum localization has been shown to set in within a few hundreds of kicks [24]. In the opposite case $\Delta p < 0$ stable islands persist, allowing for the survival of Rydberg states both classically and quantum mechanically, referred to as stabilization [22].

The unidirectional kicks build up an average field $F^{\mathrm{av}} = -\Delta p/T$. Hence, the time-periodic Hamiltonian (1) can be decomposed into the time-independent Stark Hamiltonian

$$H_{\mathrm{Stark}} = H_0 + qF^{\mathrm{av}} \tag{2}$$

plus an infinite series of harmonics of equal strength,

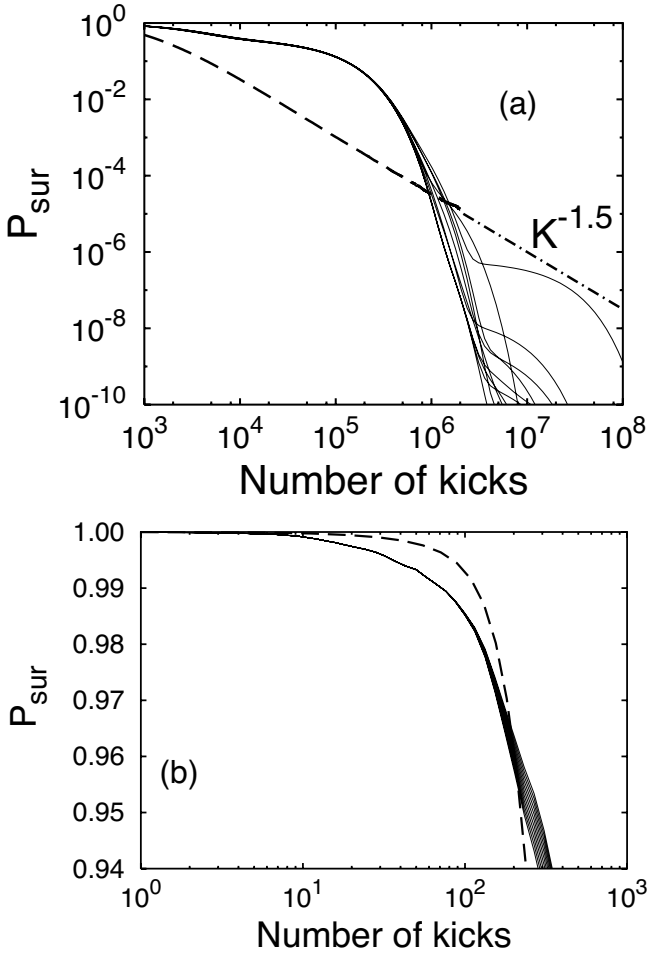

FIG. 1. Classical $P_{\mathrm{sur}}^{\mathrm{cl}}$ (dashed line) and quantum $P_{\mathrm{sur}}^{\mathrm{qm}}$ (solid lines) survival probability for the positively kicked Rydberg atom as a function of number K of kicks for $|F_0^{\mathrm{av}}|=0.005$ ($\Delta p_0 \approx 0.021$). The quantum data are shown for 11 frequencies ν_0 uniformly distributed between 1.45 and 1.45008, $n_i=50$. (a) Long-time behavior, the dash-dotted line indicates a fit to a power law with exponent $\alpha=-1.5$, Eq. (6), and (b) short-time behavior.

$$H(t) = H_{\mathrm{Stark}} + 2F^{\mathrm{av}} q \sum_{m=1}^{\infty} \cos\left[2\pi m/T\left(t-\frac{T}{2}\right)\right]. \qquad (3)$$

In this paper, we will highlight the influence of the higher harmonics $m>1$, their presence distinguishing our system from the Rydberg atom driven by a microwave field. For the "positively kicked" Rydberg atom with $\Delta p>0$ (i.e., $F^{\mathrm{av}}<0$) the Stark Hamiltonian possesses a potential barrier with maximum at $E^{\mathrm{barrier}}=-\sqrt{2|F^{\mathrm{av}}|}$ and $q^{\mathrm{barrier}}=\sqrt{1/|F^{\mathrm{av}}|}$, resulting in a finite number of quasibound states and a continuum. To keep the Stark Hamiltonian invariant—i.e. the average field fixed—we vary ν and Δp so as to keep the average field F^{av} fixed.

To calculate the long-time evolution of the quantum system we represent the period-one time-evolution operator

$$U(T) = \exp(-iH_0T/2)\exp(i\Delta pq)\exp(-iH_0T/2) \qquad (4)$$

in a basis $|n\rangle$ defined by $H_0|n\rangle=E_n|n\rangle$ by means of the pseudospectral method [25]. Dirichlet boundary conditions are applied at $q=0$ and $q=q_{\max}$. Solving the eigenvalue equation $U(T)|\phi_j\rangle=\exp(-iT\mathcal{E}_j)|\phi_j\rangle$ yields the time-dependent wave function in terms of Floquet states $|\phi_j\rangle$ as

$$|\psi(KT)\rangle = U(T)^K|\psi(0)\rangle = \sum_j d_j \exp(-iKT\mathcal{E}_j)|\phi_j\rangle, \qquad (5)$$

with $d_j=\langle\phi_j|\psi(0)\rangle$. A masking function in q is introduced to avoid spurious reflections at $q_{\max}$ (see [24]). For the low frequencies used in this paper, we apply the masking operator 3 times per period. The convergence of the wave function obtained is tested both by varying $q_{\max}$ and by comparison with direct solutions of the time-dependent Schrödinger equation (i.e., without facilitating the Floquet states ϕ_j) as described in [24,25].

For later reference we introduce scaled units, denoted by the subscript 0. They leave the classical dynamics invariant and are defined by $E_0=En_i^2$, $T_0=T/(2\pi n_i^3)$, $\nu_0=1/T_0$, and $F_0^{\mathrm{av}}=F^{\mathrm{av}}n_i^4$ where n_i is the principal quantum number (action) of the initial state [10]. Note that the transition energy due to absorption of one photon, $E_0^{\gamma}=n_i^2\hbar\omega=n_i^2 2\pi/T=\nu_0/n_i$, is *not* scaling invariant.

III. TRANSIENT QUANTUM LOCALIZATION

A. Survival probability and effective quantum number

One measure to study quantum localization is the survival probability, defined as $P_{\mathrm{sur}}(K)=\langle\psi(KT)|P_{\mathrm{bound}}|\psi(KT)\rangle$ where P_{bound} is the projection operator onto bound hydrogenic states. The underlying picture is that transport along the energy axis towards the continuum is considered to be the equivalent of conductance in disordered systems [26]. Correspondingly, suppression of energy absorption from the pulse sequence and, thus, suppression of ionization is identified as localization in a purely chaotic system or stabilization when the classical phase space is mixed.

The classical $P_{\mathrm{sur}}^{\mathrm{cl}}(K)$ is obtained by the classical trajectory Monte Carlo method (CTMC) with a microcanonical ensemble to represent the initial state [27,28]. The classical phase space (for $\Delta p>0$) is fully chaotic without any tori left intact. We show an example for the survival probability in Fig. 1. The classical $P_{\mathrm{sur}}^{\mathrm{cl}}(K)$ for times larger than K_0 kicks decays algebraically [18],

$$P_{\mathrm{sur}}^{\mathrm{cl}}(K) = (K/K_0)^{-\alpha}, \qquad (6)$$

with $\alpha \approx 1.5$. Both the time K_0 and the factor α are only weakly dependent on the parameters of the field (ν_0 and Δp_0). By contrast, the quantum survival probability $P_{\mathrm{sur}}^{\mathrm{qm}}(K)$ displays a very different and much more complex behavior. One intriguing feature is an extreme sensitivity to the driving frequency ν_0, especially in the long-time limit (compare also to the results in, e.g., [2,5,11]). The resulting fluctuations in the kicked atom will be studied below in more detail (see Sec. IV).

For characterization of quantum (de)localization it is useful to introduce another observable that describes the bound portion of the wave packet. Inspired by the relation $n=1/\sqrt{-2E}$ for bound states, we introduce a mean quantum number as

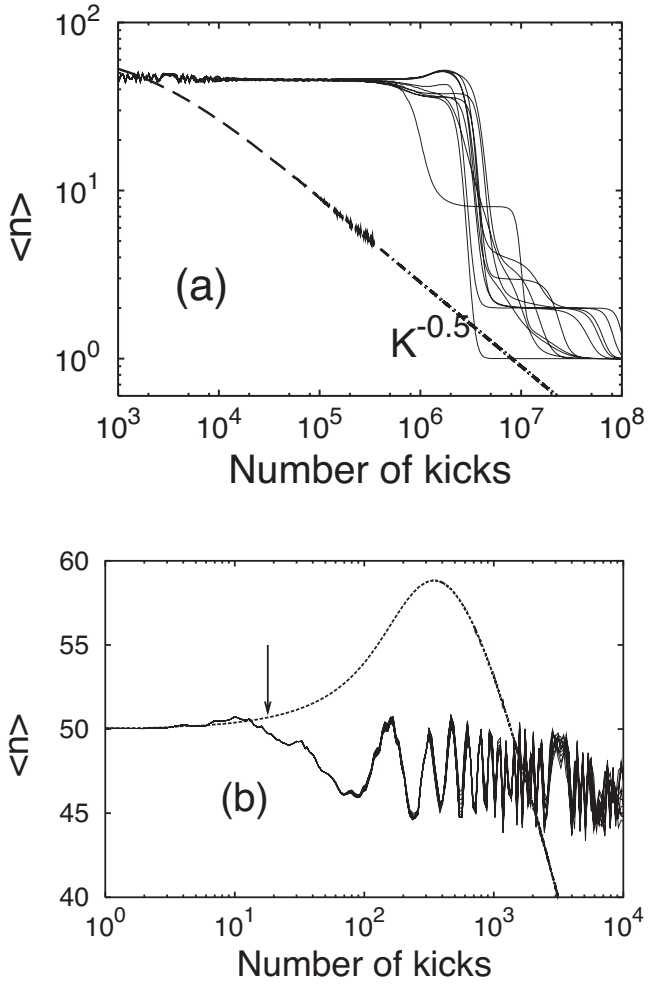

FIG. 2. Mean principal quantum number $\langle n\rangle$, Eq. (7), for the same parameters as Fig. 1, $\langle n\rangle_{\rm cl}$ (dashed line) and $\langle n\rangle_{\rm qm}$ (solid lines). (a) Long-time behavior (of $\log\langle n\rangle$), the dash-dotted line indicates a fit to a power law, and (b) short-time behavior of $\langle n\rangle$. The arrow in (b) indicates an approximate localization time defined in Eq. (16).

$$\langle n(K)\rangle = \langle \psi(KT)|P_{\rm bound}\frac{1}{\sqrt{-2H_0}}P_{\rm bound}|\psi(KT)\rangle/P_{\rm sur}(K). \tag{7}$$

In this equation, the expectation value is calculated for the portion of the wave function residing in the bound subspace. Equation (7) characterizes the specific position of that part of the wave function that remains bound, in particular that which remains localized or stabilized near the initial state (or initial torus). Indeed, $\langle n\rangle$ displays a characteristically different behavior classically $\langle n\rangle_{\rm cl}$ and quantum mechanically $\langle n\rangle_{\rm qm}$, both at short times [Fig. 2(b)] and long times [Fig. 2(a)]. The sharp drop of $\langle n\rangle_{\rm qm}$ from 50 to 1 at $K\approx 10^6$ will be analyzed in Sec. III C. The corresponding non-normalized distributions $P(n,t)$ whose mean values are given by $\langle n\rangle$ are depicted in Fig. 3. The quantum $P^{\rm qm}(n,t)$ remains well localized close to the initial state while the time evolution of $P^{\rm cl}(n,t)$ features a rapid increase of width in the energy distribution and a shift towards increasingly lower energies (i.e., smaller n).

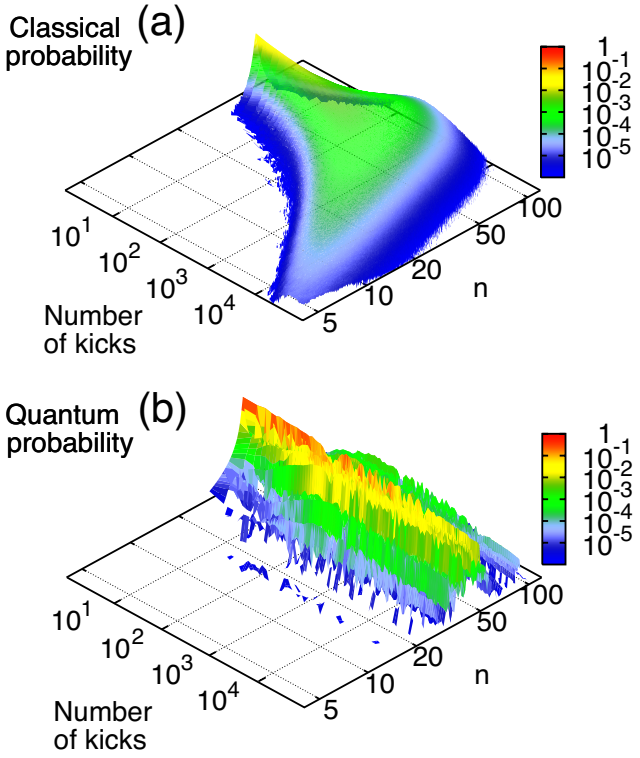

FIG. 3. (Color online) Time-dependent spectral distribution $P(n,t)$, both classically (a) and quantum mechanically (b), for the same parameters as Fig. 2 (data shown for $\nu_0=1.45$).

Note that classically n does not possess a lower bound $n=1$, as the quantum distribution does. The fact that the energy distribution can grow to negative values without bound is a root cause for the algebraic decay. The probability for crossing the $E=0$ line (i.e., the $n=\infty$ line) in the next time step and thus for reducing $P_{\rm sur}^{\rm cl}$ decreases as the mean distance to the $E=0$ line as measured by $\langle n(K)\rangle_{\rm cl}$ increases with t. We now relate the power-law decay, Eq. (6), to the motion of $P^{\rm cl}(n,t)$ away from the threshold. The classical survival probability for large times is well fitted by Eq. (6) with $K_0\approx 1000$. The scaled average quantum number is also well described by a power law,

$$\langle n_0(K)\rangle_{\rm cl} = b(K/K_0)^{-0.5}, \tag{8}$$

where the power-law decay is assumed to start at the same time as that of the survival probability and $b\approx 1.8$. The differential form of Eq. (6),

$$\frac{dP_{\rm sur}^{\rm cl}(K)}{dK} = -\frac{\alpha}{K}P_{\rm sur}^{\rm cl}(K), \tag{9}$$

can now be expressed by means of Eq. (8) as follows:

$$\frac{dP_{\rm sur}^{\rm cl}(K)}{dt} = -\frac{d}{K_0}\langle n_0(K)\rangle_{\rm cl}^2 P_{\rm sur}^{\rm cl}, \tag{10}$$

with $d=\alpha/b^2$. For some cases with stronger average fields ($F_0^{\rm av}=0.02$ and 0.05) shown in Figs. 4 and 5 (where K_0

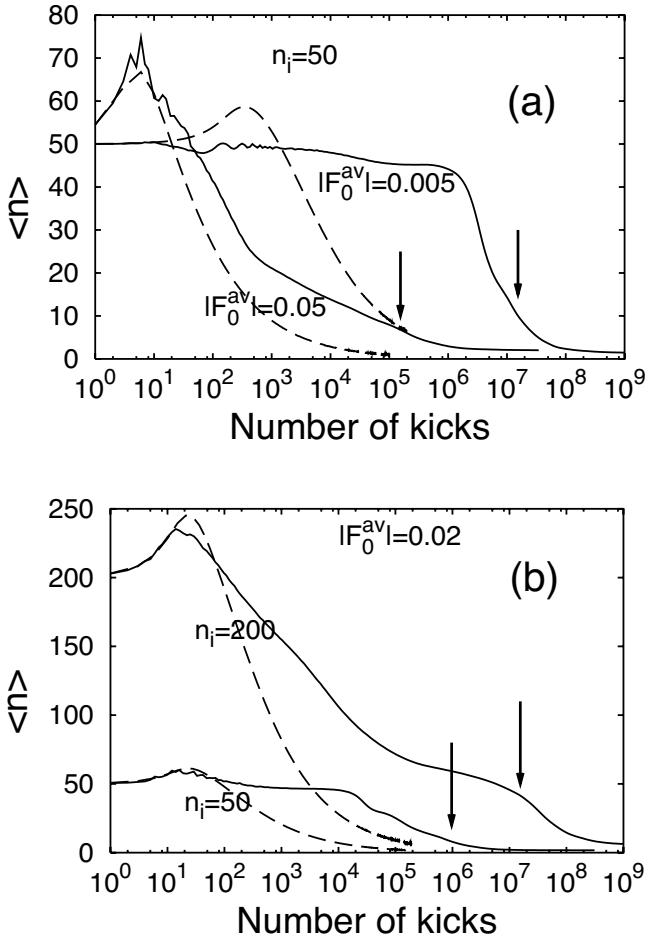

FIG. 4. $\langle n\rangle$ averaged over the interval $1.45 \leqslant \nu_0 \leqslant 1.47$. In (a), $n_i=50$, and in (b), $|F_0^{\mathrm{av}}|=0.02$. Solid line, quantum result, and dashed line, classical result. The arrows indicate the lifetimes of the ground state estimated by direct coupling to the continuum. The average is calculated on the logarithmic scale—i.e., shown is $10^{\langle \log_{10} n\rangle}$.

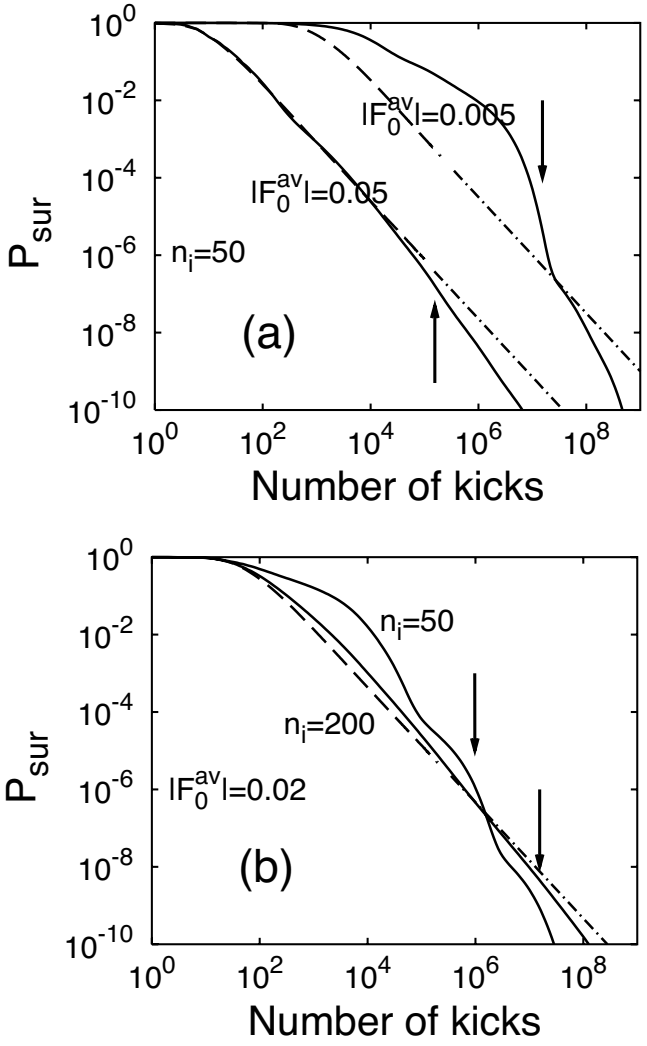

FIG. 5. P_{sur} averaged over the interval $1.45 \leqslant \nu_0 \leqslant 1.47$. In (a), $n_i=50$, and in (b), $|F_0^{\mathrm{av}}|=0.02$. Solid line, quantum result; dashed line, classical result; and dash-dotted line, fit of classical result to a power law. The arrows indicate the lifetimes of the ground state estimated by direct coupling to the continuum. The average is calculated on the logarithmic scale.

≈ 60 and 9, respectively) we find that the power law for $\langle n_0\rangle_{\mathrm{cl}}$, Eq. (8), holds with approximately the same constant b. Hence, Eq. (10) is still applicable and the constant d has essentially the same value.

We now compare the numerical signatures of quantum localization for intermediary times as seen in P_{sur}, Figs. 1(a) and 5, to the signatures seen in $\langle n\rangle$, Figs. 2(a) and 4. In all cases studied, $\langle n\rangle^{\mathrm{qm}} > \langle n\rangle^{\mathrm{cl}}$ and a clear discrepancy between the quantum and classical values can be seen for weak fields and low n_i. The discrepancy decreases as $|F_0^{\mathrm{av}}|$ or n_i increases; i.e., $\langle n\rangle^{\mathrm{qm}}$ approaches the classical limit, however quite slowly. The approach to the classical limit appears faster in P_{sur}. Here signatures of quantum localization can only be seen for weak fields and low n_i, while in the other cases shown, $P_{\mathrm{sur}}^{\mathrm{qm}}$ has already reached the classical limit. We thus conclude that the more locally focused $\langle n\rangle$ provides stronger signature of quantum localization—i.e., the suppression of diffusion away from the initial state—than the P_{sur} probing the entire bound part of phase space.

B. Short-time dynamics: The crossover to quantum localization

We take now a closer look at the short-time dynamics for the weak field strength, Figs. 1(b) and 2(b). Here a first surprise appears. One would, generally, expect $P_{\mathrm{sur}}^{\mathrm{cl}}$ and $P_{\mathrm{sur}}^{\mathrm{qm}}$ to agree with each other up to the localization time (or quantum break time, also referred to as Ehrenfest time) τ_l. The present case is nongeneric in that the classical phase-space distribution remains up to τ_l ($\approx$200 kicks) more localized when one identifies P_{sur} as a measure for localization. This quantum enhancement of ionization takes place even though the classical $\langle n\rangle_{\mathrm{cl}}$ moves closer to the ionization threshold while the quantum $\langle n\rangle_{\mathrm{qm}}$ remains close to the initial value [Fig. 2(b)]. The origin is a true quantum effect: perturbative single-photon absorption of high-frequency $m\nu_0$ from higher-harmonic components with $m \geqslant m_c(n_i)$ sufficient to reach the continuum. Here

$$m_c(n_i) = n_i/(2\nu_0). \tag{11}$$

A border for the field strength at which a single kick driving a high-lying Rydberg state displays quantum-classical correspondence can be found as follows [29]: The average classical energy transfer from a kick is

$$\Delta E_k = \Delta p_0^2. \tag{12}$$

This energy transfer can be resolved quantum mechanically if ΔE_k is not smaller than the quantum energy spacing $\Delta E_{n_i}^0 = 1/n_i$, leading to the critical momentum transfer

$$\Delta p_0^{\text{crit}} = 1/\sqrt{n_i}. \tag{13}$$

For $\Delta p_0 > \Delta p_0^{\text{crit}}$, the quantum and classical distributions after a single kick agree all the way up to the threshold $E=0$ since the quantum-level spacing decreases as $n \to \infty$, and good agreement between the quantum and classical survival probabilities is achieved. The difference between the classical and quantum distributions for $\Delta p_0 < \Delta p_0^{\text{crit}}$ can be understood by considering the dipole limit $\Delta p_0 < \Delta p_0^{\text{dipole}} = 1/n_i$, for which the transition operator for a single kick, $\exp(i\Delta pq)$, reduces to

$$\exp(i\Delta pq) \approx 1 + i\Delta p_0 q_0 n_i + \cdots. \tag{14}$$

In this limit, the quantum transition amplitude is proportional to Δp and the probability is proportional to Δp^2. By contrast, the classical probability is proportional to Δp^5, implying that the quantum survival probability after one kick is smaller than the classical one [29]. Physically, this can be understood by considering the Fourier transform of a delta kick,

$$\delta(t - t_0) = \frac{1}{2\pi}\int_{\infty}^{\infty} d\omega \exp[i\omega(t - t_0)], \tag{15}$$

indicating a "white" spectrum. The quantum system can absorb (virtual) photons of arbitrarily high frequency from the white spectrum accompanied by only a small momentum transfer $\Delta p_0 \ll 1$. Processes with large energy transfer $\Delta\omega_0 \gg 1$ but small momentum transfer Δp_0 are far from the line $\Delta\omega_0 \approx \Delta p_0^2/2$ in the $\Delta\omega_0 - \Delta p_0$ dispersion plane for a quasifree electron and thus effectively are inaccessible for a classical momentum transfer process. Only for deeply bound electrons with large local orbital momentum p_0 near the nucleus, with $\Delta\omega_0 \approx p_0 \Delta p_0 \gg \Delta p_0^2/2$, can such processes occur in the classical case. The density of classical phase-space points for the initial state with such high p_0 is, however, very small. In the quantum case, the high-frequency components in the driving field interact nonlocally with the whole initial state, leading to an enhanced ionization probability. This corresponds to dipole-allowed transitions. Classical-quantum correspondence is only restored when classical diffusion in phase space dominates the quantum enhancement due to (virtual) photon absorption.

For $n_i=50$ and $\nu_0=1.45$ the corresponding critical fields are $|F_0^{\text{crit}}|=0.033$ and $|F_0^{\text{dipole}}|=0.0047$; i.e., the cases studied in Figs. 1 and 2 are close to the dipole limit. The important point is that the dynamical role of the high-harmonics spectrum of (virtual) photons is responsible for the surprising, nongeneric features of the periodically kicked Rydberg atom,

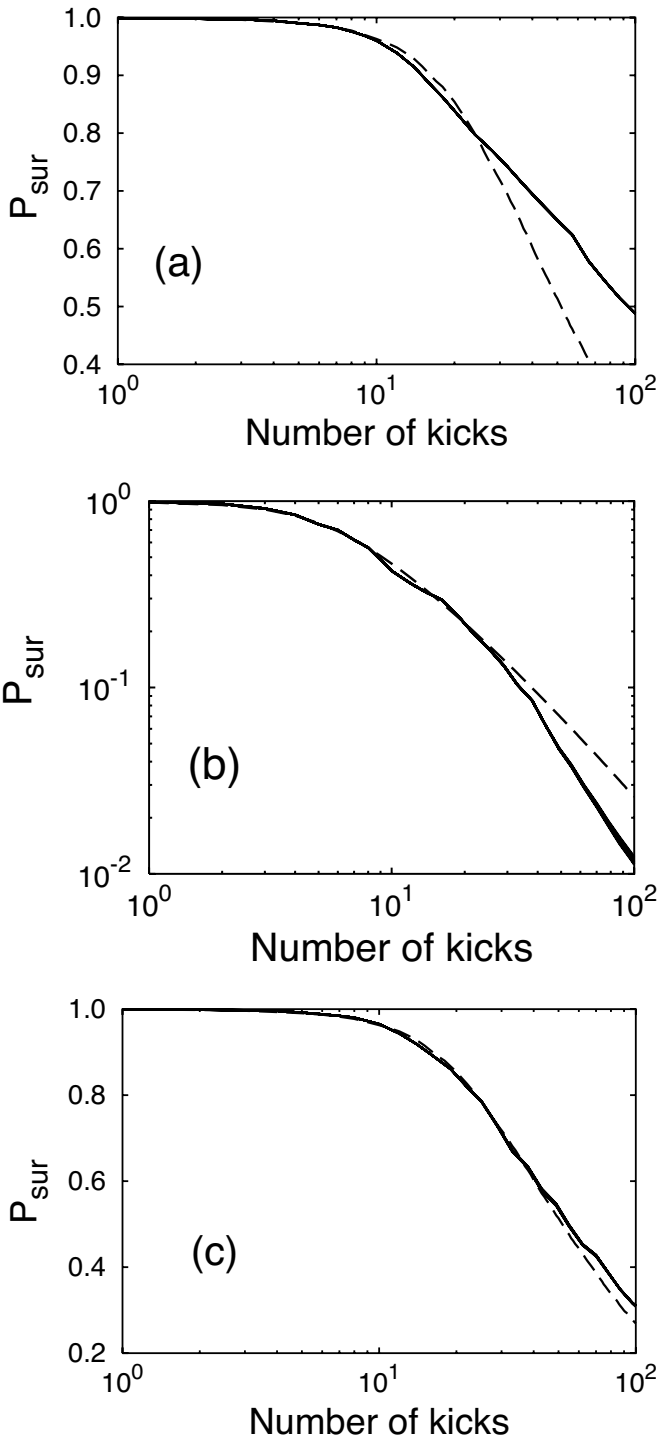

FIG. 6. As Fig. 1(b), however for (a) $|F_0^{\text{av}}|=0.02$ and $n_i=50$, (b) $|F_0^{\text{av}}|=0.05$ and $n_i=50$, and (c) $|F_0^{\text{av}}|=0.02$ and $n_i=200$.

different from other systems such as the Rydberg atom in a microwave field. This is directly verified by increasing the field such that the scaled momentum transfer $\Delta p_0 \approx \Delta p_0^{\text{crit}}$; see Fig. 6. We show first a case in the transition region ($|F_0^{\text{av}}|=0.02$, $n_i=50$) where still some traces of the nongeneric features at short times can still be seen. For larger n_i or larger $|F_0^{\text{av}}|$ such that $\Delta p_0 > \Delta p_0^{\text{crit}}$ the quantum-classical agreement for short times is quite well fulfilled while discordance is

found only for larger times $t > \tau_l$. The short-time dynamics now conforms with the naive expectation of close classical-quantum correspondence for all $t < \tau_l$.

Well-known arguments [30] for the localization time lead to the order-of-magnitude estimate

$$\tau_l \approx \frac{1}{\langle L \rangle} \ln\left(\frac{\langle q \rangle}{\lambda_i}\right), \tag{16}$$

where $\langle q \rangle = n_i^2$ is the typical spatial extension of the initial state, $\lambda_i = n_i$ the wavelength of the initial state, and $\langle L \rangle$ the mean Lyaponov exponent. τ_l is indicated by arrows in Figs. 2(b) and 7. For $\langle n \rangle$, τ_l gives a reasonable estimate for the number of kicks up to where quantum and classical dynamics mirror each other.

The situation for the survival probability is more involved: For $\Delta p_0 < \Delta p_0^{\text{crit}}$, Eq. (13) [see Figs. 1 and 6(a)], no agreement between $P_{\text{sur}}^{\text{cl}}$ and $P_{\text{sur}}^{\text{qm}}$ is found for short times and a break time τ_l now defined as the time where $P_{\text{sur}}^{\text{cl}}$ gets smaller than $P_{\text{sur}}^{\text{qm}}$ due to quantum localization takes on a different meaning. Consequently, this break time is not well described by Eq. (16). For the cases with $\Delta p_0 > \Delta p_0^{\text{crit}}$ [Figs. 5, 6(b), and 6(c)] we find no clear numerical signatures of localization in P_{sur}.

C. Long-time dynamics: The second crossover

Quantum localization in the kicked Rydberg atom is transient. After a large but finite number of kicks [Figs. 1(b) and 6], the quantum survival probability rapidly decreases and at a second crossover time (delocalization time) τ_D falls below even the classical value. Simultaneously, $\langle n \rangle_{\text{qm}}$ drops sharply from values near n_i to 1 [Figs. 2(b) and 7(b)]. Beyond the crossover point, $\langle n \rangle_{\text{cl}}$ falls to values well below unity inaccessible to quantum mechanics. There, the residual fraction of the classical phase is "sheltered" and continues to decay slowly—i.e., algebraically. By contrast, the quantum bound-state probability decays exponentially in the long-time limit. Beyond τ_D the slow classical algebraic decay "wins" over the exponential decay. This novel scenario is markedly different from the sinusoidal driven Rydberg atom, where the quantum transport is bounded from below because of the regular phase-space region or, in a quantum picture, because of vanishingly small transition probabilities to states with low principal quantum numbers [2,10,31].

The rate of the long-time decay and, thus, of τ_D can be estimated from the decay rate of the state $n=1$ due to the high harmonics. This is the lowest-lying and most stable component of any coherent superposition forming a Floquet state. All frequencies of the driving field, Eq. (3), with scaled energy $m\nu_0$ large enough to couple the Stark state having the largest overlap with the $n=1$ hydrogenic state to the Stark continuum contribute to the transition probability according to Fermi's golden rule,

$$\Gamma_m = 2\pi\rho(E_m)|F^{\text{av}} z(n=1, E_m)|^2, \tag{17}$$

with $E_m = -1/2 + m\nu_0/n_i^3$. Both dipole matrix elements $z(n,E)$ and the density of continuum states $\rho(E)$ are numerically obtained by diagonalizing the Stark Hamiltonian (2) in the pseudospectral basis. Summing over all contributions leads to a delocalization time $\tau_D = (\Sigma_m \Gamma_m)^{-1}$ which corresponds to within a factor of 2 to the lifetime of the most long-lived Floquet state with $\langle n \rangle \approx 1$. $\langle n \rangle_{\text{qm}}$ averaged over an interval in ν $(1.45 \leqslant \nu_0 \leqslant 1.47)$ together with the estimated τ_D is shown in Fig. 4. τ_D clearly gives a good estimate of the time scale on which the breakdown of quantum localization as seen in $\langle n \rangle$ takes place. The estimated τ_D also coincide

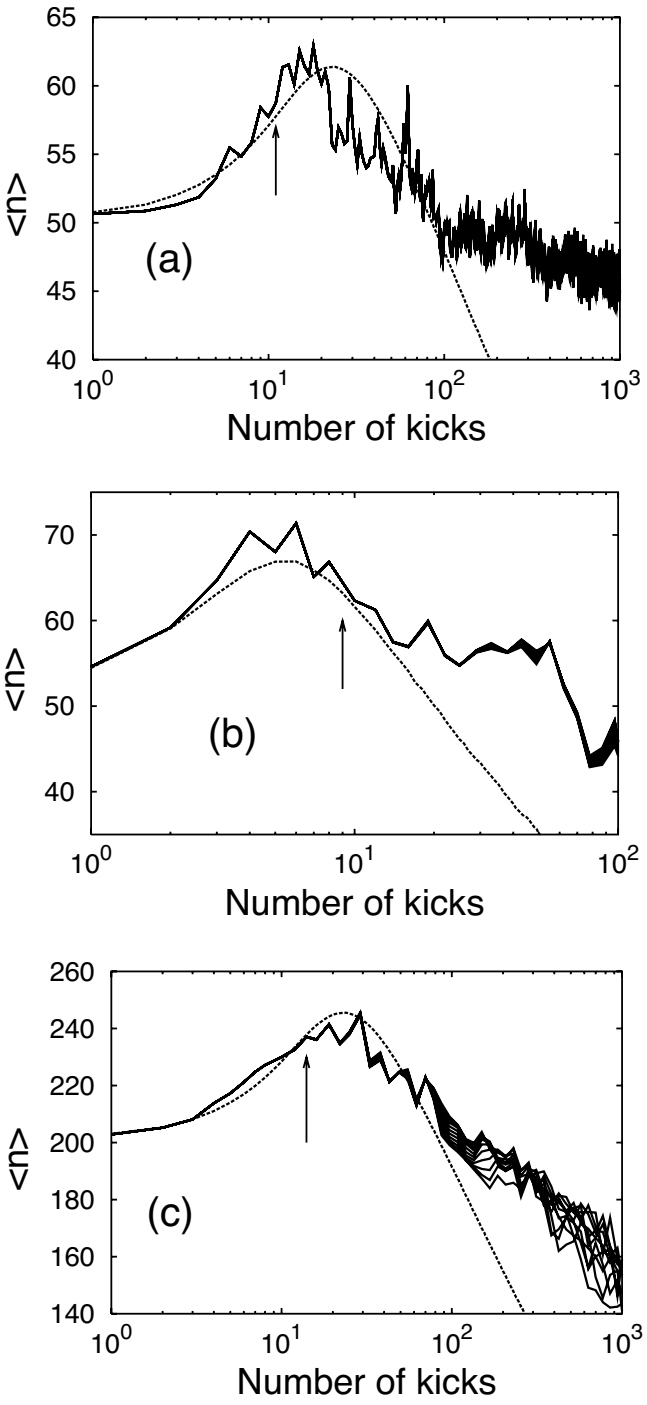

FIG. 7. As Fig. 2(b), however for (a) $|F_0^{\text{av}}| = 0.02$ and $n_i = 50$, (b) $|F_0^{\text{av}}| = 0.05$ and $n_i = 50$, and (c) $|F_0^{\text{av}}| = 0.02$ and $n_i = 200$. The arrows indicate an approximate localization time defined in Eq. (16).

with $P_{\mathrm{sur}}^{\mathrm{qm}}$ getting smaller than the classical value (Fig. 5). We thus attribute the breakdown of quantum localization to the higher harmonics in the driving field. The breakdown of localization is expected if the ground state $n=1$ is directly coupled to the continuum. We note parenthetically that an experimental realization would require half-cycle pulses with high-frequency components in the UV region. Work is currently under way on a protocol to produce half-cycle pulses in the attosecond regime [32].

We now comment on the decay of the quantum survival probability for $|F_0^{\mathrm{av}}|=0.005$ and 0.02, $n_i=50$, seen for intermediate times [$K<10^6$ and 10^4 in Figs. 5(a) and 5(b), respectively]. Here $\langle n\rangle^{\mathrm{qm}} \approx n_i$ (Fig. 4), indicating the localization of the quantum distribution $P(n,t)^{\mathrm{qm}}$ [see also Fig. 3(b)]. As for $\langle n\rangle$, Eq. (7), we attribute the decay of the localized bound part of the quantum wave function in the kicked atom to the higher harmonics present in the driving field, directly coupling the wave packet localized close to the initial state with the continuum.

IV. FLUCTUATIONS IN THE SURVIVAL PROBABILITY

The quantum survival probability shown in Fig. 1 displays strong fluctuations under small variations of the kick frequency. Such fluctuations are a direct consequence of the photonic localization scenario [2,8,11], to be described in the following.

A. High harmonics in the localization regime

The observation of localization—i.e., the suppression of ionization or, equivalently, the freezing out of portions of the wave function near n_i—raises the question as to the underlying mechanism in the presence of the harmonic spectrum [Eq. (3)]. High harmonics cannot only directly couple to the continuum (see Sec. III C), but they also can lead to sequential excitation through a ladder of intermediate (quasi)bound states. This channel is the dominant mechanism for the excitation and ionization by the harmonic driving by the lowest harmonic ν_0. Jensen *et al.* [8] have discussed the suppression of the sequential ladder excitation by a harmonic driving as a mechanism for localization ("photonic localization"). It is therefore instructive to extend this approach to the present multiphoton case.

Following [8] we assume quasiresonant one-photon transitions to dominate the time evolution; i.e., we consider only transition between (bound) states with energy differences to the initial state approximately equal to k times the fundamental photon energy $E_0^{\gamma}=\nu_0/n_i$. The detunings

$$\Delta_k = E_k - E_{n_i} - k\nu \tag{18}$$

for the quasiresonant states $|k\rangle$ form a pseudorandom sequence of numbers. Using the rotating-wave approximation and setting $c_k(t)=b_k(t)\exp(-i\Delta_k t)$, with $b_k(t)$ the expansion coefficient for the kth quasiresonant state in the interaction picture, leads to a set of coupled differential equations

$$i\frac{dc_k}{dt} = \sum_{k'} H_{kk'}^J c_{k'}, \tag{19}$$

with the matrix H^J given by

$$H_{kk'}^J = \Delta_k \delta_{kk'} + V_{k,k'}. \tag{20}$$

The semiclassical expression for the coupling matrix elements is [8]

$$V_{kk'} \approx 0.411F/[(n_k n_{k'})^{3/2}(m\nu_0)^{5/3}], \tag{21}$$

with $m=|k-k'|$ and n_k the main quantum number of the kth quasiresonant state. While for the harmonically driven case $V_{kk'}\neq 0$ only for $m=1$, the coupling matrix elements for the periodically kicked Rydberg atom in the mth off diagonal are proportional to $m^{-5/3}$. Due to the randomness of the detunings Δ_k, the matrix H^J is thus a pseudorandom, power-law banded matrix. In random power-law banded matrices with the elements decreasing as $m^{-\beta}$, the eigenstates are (weakly) localized for $\beta \geqslant 1$ [33]. Our extension of the model introduced in [8] on the basis of [2] thus predicts that the eigenstates for the kicked Rydberg atom should be localized. Inferring from the numerical observation of quantum localization that the detunings are "sufficiently" random, the generalization of the photonic localization scenario appears applicable.

We finally comment on the (semi)classical border $n_i \to \infty$. Increasing n_i from 50 to 200, the quantum localization for $|F_0^{\mathrm{av}}|=0.02$ almost vanishes [Figs. 4(b) and 5(b)]. This indicates that a delocalization border is present in the kicked atom similar to that found for the harmonically driven system [2]. The presence of a delocalization border implies a maximum n_i for the applicability of the photonic localization theory. Detailed studies of this border in the kicked Rydberg atom remain to be performed.

B. Characterization of parametric fluctuations

We turn now to a quantitative description of the parametric fluctuations of $P_{\mathrm{sur}}^{\mathrm{qm}}$ under variation of ν_0 seen in Fig. 1. Figure 8 displays the evolution towards an increasingly complex fluctuation pattern as K increases. The amplitudes of the fluctuations increase by several orders of magnitude. Strong fluctuations in the survival probability have also been found, e.g., in the harmonically driven Rydberg atom [11] and in the kicked rotor when subjected to a varying Aharonov-Bohm flux [34] or a variation of the kicking frequency [35].

In order to characterize the increasingly finer scale on which these fluctuations occur, we determine the average distance between adjacent maxima and minima on the frequency scale $\langle \delta_{\nu_0}(K)\rangle$. At times smaller than the delocalization time τ_D, $\langle \delta_{\nu_0}(K)\rangle$ is rapidly decreasing (Fig. 9). A similar buildup of fluctuations in the survival probability with time is observed for the kicked rotor [35]. In the very-long-time limit beyond τ_D, where the dynamics of the kicked system is governed by the decay of the ground state, no further fluctuations are produced but $\langle \delta_{\nu_0}(K)\rangle$ saturates.

It is now tempting to inquire whether the complexity of the fluctuations in the $P_{\mathrm{sur}}^{\mathrm{qm}}$ can be described by an approximate fractal dimension. For example, the fluctuations in the kicked rotor in the chaotic regime have been shown to have a fractal structure [34,35]. Fractal conductance fluctuations have been predicted [36] and experimentally found—e.g., [37]—for the transport through cavities with mixed classical

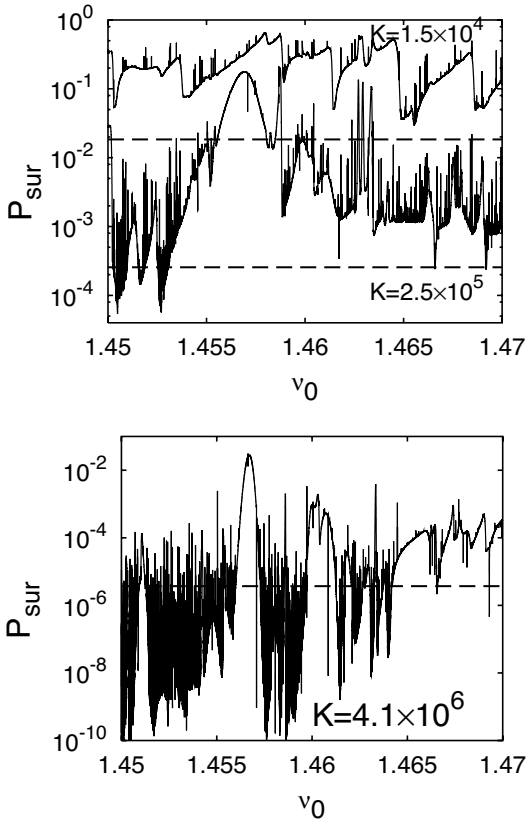

FIG. 8. Survival probability P_{sur} versus frequency ν for some numbers K of kicks. $n_i=50$ and $|F_0|^{\mathrm{av}}=0.005$. The dashed lines give the classical results.

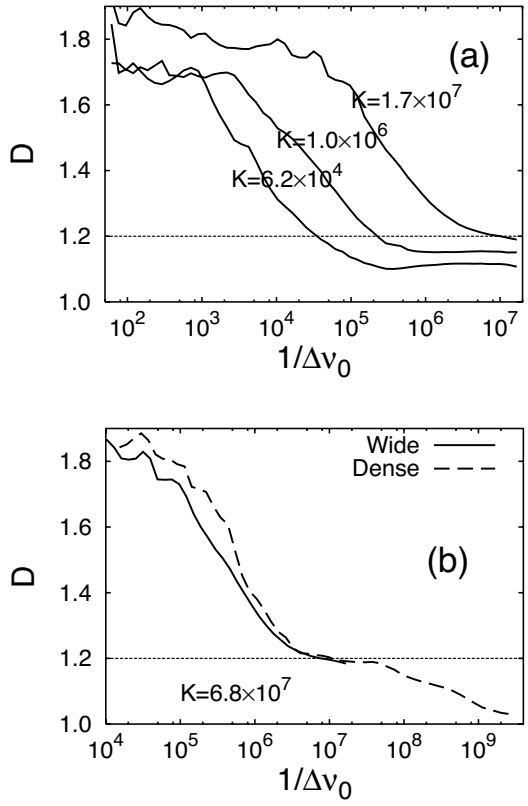

FIG. 10. Fractal analysis of $\log_{10}(P_{\mathrm{sur}})$ for $n_i=50$ and $|F_0^{\mathrm{av}}|=0.005$. In (a) we show the data analyzed for 2×10^6 points in the interval $1.45\leqslant\nu_0\leqslant1.47$ for different numbers K of kicks, and in (b) we combine the wide set of (a) with data for a dense set containing 10^6 points in the interval $1.45\leqslant\nu_0\leqslant1.45008$ for $K=6.8\times10^7$.

phase space. A fractal structure has also been found in the survival probability of a system with a mixed phase space [38]. In both cases, a semiclassical explanation based on a classical power-law decay has been proposed. Since the kicked Rydberg atom displays classically such a power-law decay even though its phase space is fully chaotic, rather than mixed, a fractal is a conceivable candidate.

For a given "resolution" $\Delta\nu_0$ in frequency we calculate the local fractal dimension $D(\Delta\nu_0)$ by means of a variational method [39]. Rigorously, this value should be independent of

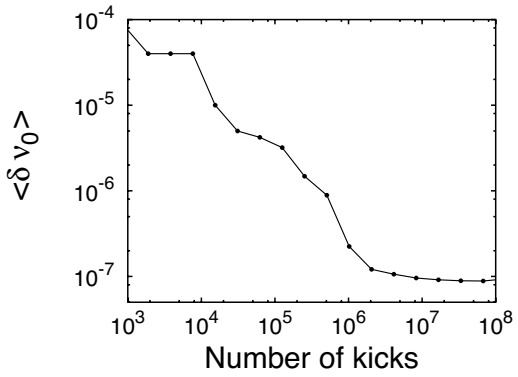

FIG. 9. Average distance $\langle\delta_{\nu_0}(K)\rangle$ between extrema in P_{sur} as a function of number K of kicks. $n_i=50$ and $|F_0^{\mathrm{av}}|=0.005$. We analyze a set containing 10^6 points on $1.45\leqslant\nu_0\leqslant1.45008$.

$\Delta\nu_0$. In the present physical context, we are satisfied if $D(\Delta\nu_0)$ is approximately constant over at least one order of magnitude in $\Delta\nu_0$. The fractal analysis of the data shown in Fig. 8 is presented in Fig. 10(a). Since the survival probability fluctuates over many orders of magnitude, we analyze the logarithm of the data. After more than 10^5 kicks, a plateau starts to develop, the width of which reaches almost two orders of magnitude for larger K. The value of D on the plateau increases with K up to about $D\approx1.2$. The process of increasingly finer rescaling is transient and stops beyond $K>10^7$ when τ_D is reached. Zooming in on a narrow frequency interval for $K>K_D$ [Fig. 10(b)], the plateau value is still $D\approx1.2$, but the width of the plateau is only about one order of magnitude. Thus, a tendency towards a noninteger dimension can be found in the positively kicked Rydberg atom. The value is weakly dependent on the number K of kicks for which the fractal analysis is made and appears to approach $D\approx1.2$.

It is now instructing to compare this value with the semiclassical prediction [36,38,40] based on the power-law decay with exponent $\alpha=1.5$ (see Fig. 1) of the classical survival probability $P_{\mathrm{sur}}^{\mathrm{cl}}(K)$, $D_{\mathrm{SC}}=2-\alpha/2=1.25$. The value for D_{SC} is remarkably close to the plateau value found from the fractal dimension analysis. We thus conclude that the onset of a self-similar fluctuation pattern can be observed with a dimension close to the semiclassical prediction derived from

the classical power-law decay. We note that this process is transient in that the finest scale for the fluctuations is determined by the time τ_D beyond which the most stable bound state decays.

V. SUMMARY

We have studied the long-time limit of quantum localization of the positively kicked Rydberg atom, involving clear signatures of a quantum suppression of classical ionization. We compare the localization as seen in the survival probability to that seen in an average quantum number $\langle n \rangle$ describing the position of the localized part of the wave function [see Eq. (7)]. In $\langle n \rangle$ clearer signatures of quantum localization prevailing to higher field strengths and larger quantum numbers are found. Two crossover times could be identified: the crossover from classical-quantum correspondence to localization (τ_l) and the destruction or delocalization at a much later time (τ_D). Remarkably, beyond τ_D, the quantum system decays faster then the classical counterpart due to direct transitions to the continuum resembling photoionization. This process, identified in the present paper within a 1D model, is expected to be operative in a full 3D model as well. Quantum localization is accompanied by strong fluctuations in the survival probability after a given number of kicks as a function of the frequency of the driving field. The average distance between the fluctuations $\langle \delta_{\nu_0}(t) \rangle \propto 1/t$ until $t = \tau_D$, whereafter $\langle \delta_{\nu_0} \rangle$ saturates. In the localization regime, the complex fluctuation pattern approaches a fractal.

In this paper we have highlighted effects caused by the higher harmonics in the driving field distinguishing the kicked atom from the Rydberg atom driven by a microwave field. Further studies comparing these two systems, including an assessment on how closely the quantum localization in the kicked Rydberg atom is related to Anderson localization using, e.g., the methods in [2,11], is left for forthcoming studies.

ACKNOWLEDGMENTS

This work was supported by the FWF (Austria) under Grant No. SFB-016. Discussions with Andreas Buchleitner and Shuhei Yoshida are gratefully acknowledged.

[1] H.-J. Stöckmann, *Quantum Chaos: An Introduction* (Cambridge University Press, Cambridge, England, 1999).
[2] G. Casati, B. V. Chirikov, and D. L. Shepelyansky, Phys. Rep. **154**, 77 (1987); G. Casati, I. Guarneri, and D. L. Shepelyansky, IEEE J. Quantum Electron. **24**, 1420 (1988).
[3] M. V. Berry, Physica D **33**, 26 (1988).
[4] G. Casati, B. V. Chirikov, F. M. Izraelev, and J. Ford, Lect. Notes Phys. **93**, 334 (1979); G. Casati, I. Guarneri, and D. L. Shepelyansky, Phys. Rev. Lett. **62**, 345 (1989).
[5] S. Fishman, D. R. Grempel, and R. E. Prange, Phys. Rev. Lett. **49**, 509 (1982).
[6] S. Adachi, M. Toda, and K. Ikeda, Phys. Rev. Lett. **61**, 659 (1988).
[7] F. L. Moore, J. C. Robinson, C. F. Bharucha, B. Sundaram, and M. G. Raizen, Phys. Rev. Lett. **75**, 4598 (1995).
[8] R. V. Jensen, S. M. Susskind, and M. M. Sanders, Phys. Rep. **201**, 1 (1991).
[9] J. E. Bayfield and L. A. Pinnaduwage, Phys. Rev. Lett. **54**, 313 (1985).
[10] P. M. Koch and K. A. H. van Leeuwen, Phys. Rep. **255**, 289 (1995).
[11] A. Buchleitner, I. Guarneri, and J. Zakrzewski, Europhys. Lett. **44**, 162 (1998); S. Wimberger and A. Buchleitner, J. Phys. A **34**, 7181 (2001).
[12] A. Buchleitner, D. Delande, J. Zakrzewski, R. N. Mantegna, M. Arndt, and H. Walther, Phys. Rev. Lett. **75**, 3818 (1995).
[13] J. Leopold and D. Richards, J. Phys. B **22**, 1931 (1989).
[14] R. R Jones, D. You, and P. H. Bucksbaum, Phys. Rev. Lett. **70**, 1236 (1993).
[15] M. T. Frey, F. B. Dunning, C. O. Reinhold, and J. Burgdörfer, Phys. Rev. A **53**, R2929 (1996).
[16] J. Bromage and C. R. Stroud, Phys. Rev. Lett. **83**, 4963 (1999).
[17] J. Burgdörfer, Nucl. Instrum. Methods Phys. Res. B **42**, 500 (1989); M. Melles, C. O. Reinhold, and J. Burgdörfer, *ibid.* **79**, 109 (1993).
[18] C. F. Hillermeier, R. Blümel, and U. Smilansky, Phys. Rev. A **45**, 3486 (1992).
[19] M. Klews and W. Schweizer, Phys. Rev. A **64**, 053403 (2001).
[20] J. Ahn, D. N. Hutchinson, C. Rangan, and P. H. Bucksbaum, Phys. Rev. Lett. **86**, 1179 (2001); T. J. Bensky, M. B. Campbell, and R. R. Jones, *ibid.* **81**, 3112 (1998).
[21] C. Wesdorp, F. Robicheaux, and L. D. Noordam, Phys. Rev. Lett. **87**, 083001 (2001).
[22] S. Yoshida, C. O. Reinhold, and J. Burgdörfer, Phys. Rev. Lett. **84**, 2602 (2000); S. Yoshida, C. O. Reinhold, P. Kristöfel, and J. Burgdörfer, Phys. Rev. A **62**, 023408 (2000).
[23] C. O. Reinhold, W. Zhao, J. C. Lancaster, F. B. Dunning, E. Persson, D. G. Arbó, S. Yoshida, and J. Burgdörfer, Phys. Rev. A **70**, 033402 (2004).
[24] E. Persson, S. Yoshida, X.-M. Tong, C. O. Reinhold, and J. Burgdörfer, Phys. Rev. A **68**, 063406 (2003).
[25] X. M. Tong and S. I. Chu, Chem. Phys. **217**, 119 (1997); J. Wang, Shih-I. Chu, and C. Laughlin, Phys. Rev. A **50**, 3208 (1994).
[26] F. Borgonovi, I. Guarneri, and L. Rebuzzini, Phys. Rev. Lett. **72**, 1463 (1994).
[27] R. Arbines and I. C. Percival, Proc. Phys. Soc. London **88**, 861 (1966).
[28] C. O. Reinhold, J. Burgdörfer, M. T. Frey, and F. B. Dunning, Phys. Rev. Lett. **79**, 5226 (1997); M. T. Frey, F. B. Dunning, C. O. Reinhold, S. Yoshida, and J. Burgdörfer, Phys. Rev. A **59**, 1434 (1999).
[29] C. O. Reinhold and J. Burgdörfer, J. Phys. B **26**, 3101 (1993).
[30] I. L. Aleiner and A. I. Larkin, Phys. Rev. B **54**, 14423 (1996).
[31] S. Wimberger, A. Krug, and A. Buchleitner, Phys. Rev. Lett.

89, 263601 (2002).
[32] E. Persson, K. Schissl, A. Scrinzi, and J. Burgdörfer, Phys. Rev. A **74**, 013818 (2006).
[33] A. D. Mirlin, Y. V. Fyodorov, F.-M. Dittes, J. Quezada, and T. H. Seligman, Phys. Rev. E **54**, 3221 (1996).
[34] G. Benenti, G. Casati, I. Guarneri, and M. Terraneo, Phys. Rev. Lett. **87**, 014101 (2001).
[35] A. Tomadin, R. Mannella, and S. Wimberger, J. Phys. A **39**, 2477 (2006).
[36] R. Ketzmerick, Phys. Rev. B **54**, 10841 (1996); A. S. Sachrajda, R. Ketzmerick, C. Gould, Y. Feng, P. J. Kelly, A. Delage, and Z. Wasilewski, Phys. Rev. Lett. **80**, 1948 (1998).
[37] H. Hegger, B. Huckestein, K. Hecker, M. Janssen, A. Freimuth, G. Reckziegel, and R. Tuzinski, Phys. Rev. Lett. **77**, 3885 (1996).
[38] G. Casati, I. Guarneri, and G. Maspero, Phys. Rev. Lett. **84**, 63 (2000).
[39] B. Dubuc, J. F. Quiniou, C. Roques-Carmes, C. Tricot, and S. W. Zucker, Phys. Rev. A **39**, 1500 (1989).
[40] Y.-C. Lai, R. Blümel, E. Ott, and C. Grebogi, Phys. Rev. Lett. **68**, 3491 (1992).